# Impurity transport driven by trapped-particle turbulence in tokamak plasmas

M. Lesur[1], E. Gravier[1], K. Lim[1], C. Djerroud[1], M. Idouakass[2], X. Garbet [3], Y. Sarazin[3]

[1] *Université de Lorraine, CNRS, IJL, F-54000 Nancy, France*

[2] *National Institute for Fusion Science, NINS, Toki, Japan*

[3] *CEA, IRFM, F-13108, Saint-Paul-Lez-Durance, France*

Impurities in magnetic confinement fusion plasmas are all ion species except for hydrogen isotopes. We aim at improving theoretical understanding of impurity transport in order to mitigate their accumulation in the core (to avoid fuel dilution and radiative losses) and eject helium ashes. The transport of impurities originates from MHD modes, collisions and turbulence. In this paper we focus on the latter. Since turbulent transport is sensitive to kinetic and non-local effects, we use global gyrokinetic simulations. To limit computing time, we choose the gyrobounce gyrokinetic code TERESA, and we focus on deeply-trapped particles (here trapped refers to the trapping by the magnetic field in a torus). The trajectories of these particles can be described in a 2D phase-space parametrized by an energy invariant. The TERESA code was designed to investigate instabilities, turbulence and transport in collisionless trapped-particle-driven turbulence.

The role of kinetic effects in general was discussed in Refs. [1, 2, 3]. TERESA was applied in 2018 to a deuterium plasma with non-trace concentrations of tungsten, showing that peaked or hollow impurity density profile can change the nature of turbulence from TEM to TIM [4]. This paper focuses on more recent simulations with deuterium and impurities, to investigate the impacts of impurity concentration, charge, mass and gradients.

**Impact of non-trace concentrations**

Trace impurities can be treated either *actively* (or self-consistently) or *passively* (as test particles, neglecting their impact on the electromagnetic field). The latter approach is valid for low enough concentrations. The contribution (on the field) of impurity charge density scales as $CZ^2$, where $C$ is the impurity concentration, and $Z$ its charge number. In order of magnitude, the trace limit is to $CZ^2 \ll 1$. In Ref. [5], which we summarize here, we describe the impacts of impurity, on impurity transport, as a function of its concentration, including for concentrations $C > 1/Z^2$.

This analysis is based on a series of hundreds of simulations with active (self-consistent) treatment of impurities, and comparisons with another series of simulations with passive (test-particle) treatment of impurities. The results depend on the ratio between density gradient and

temperature gradient [5]. Here we focus on a case with equal gradients.

Fig. 1 summarizes the impact of $W^{40+}$ concentration. It shows variations of key quantities due to impurity normalised to the value without impurity. For example, the relative variation of linear growth rate $\gamma$ is defined as $(\gamma-\gamma_0)/\gamma_0$, where $\gamma_0$ is the growth rate when $C=0$. A similar definition is used for turbulence intensity. As for the impurity density flux, it is priorly normalised to $C$, and the variation is with respect to the impurity flux in the trace limit. For $C<5\times10^{-4}$ (i.e. $CZ^2<0.8$), the observed variation of linear growth rate against impurity concentration agrees with an analytic expression (cf. appendix 1 of Ref. [5]). It was already shown in Refs. [6, 7] that impurities stabilize the trapped-electron-mode. However, conversely to the explanation proposed in Refs. [6, 7], we found that this is mainly due to an increasing contribution of the adiabatic response of passing impurities in the quasi-neutrality equation when $CZ^2\sim1$.

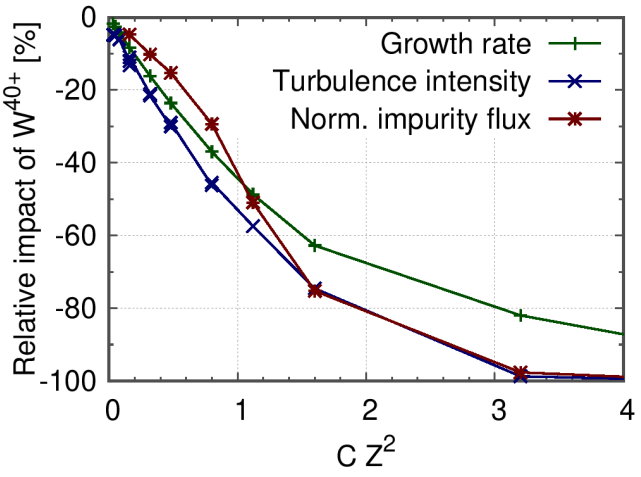


Figure 1: *Relative variation with respect to tungsten concentration of linear growth-rate, turbulent intensity and density flux.*

The observed variation of turbulence intensity against impurity concentration is in qualitative agreement with the mixing length estimate $e\phi/T_0=\gamma/(k_r\rho_{c,i}k_\theta c_s)$. However, quantitatively, the latter expression underpredicts the impact of concentration.

Most strikingly, the variation of impurity density flux against impurity concentration does not simply follow that of the turbulence intensity. The behavior is more threshold-like, as can be seen in Fig. 1 by comparing the steepness of the three curves around $CZ^2=1.1$. This threshold is also the limit between passive and active behavior of the impurity of validity of the passive treatment. Hence, in this case of equal density and temperature gradient, we warn against adopting a passive approach for $W^{40+}$ concentrations above $2\times10^{-4}$. If the density profile is flat, we obtain qualitatively similar results, albeit for the heat flux. The validity of passive treatment is then $C<10^{-4}$.

In Ref. [5], we further analyse the transition between passive and active behavior, indicating phase-synchronization between impurity density fluctuations and electric potential fluctuations for high enough impurity concentrations, which quenches impurity transport. Here we focused on tungsten. Similar results for carbon are described in the reference.

**Diffusion, thermo-diffusion, and curvature pinch**

Hereafter, the impurity species are treated self-consistently but in the trace limit, so that impurity concentrations do not affect the nature of the turbulence. The impurity flux can be written as

$$\Gamma_Z = -D_Z \frac{\partial n_Z}{\partial r} + n_Z V_Z = -D_Z \left( \frac{\partial n_Z}{\partial r} + C_T \frac{\partial T_Z}{\partial r} + C_P \frac{\partial q}{\partial r} \right) \quad (1)$$

where $D_Z$ may be then assumed as independant from impurity concentration and profiles (but not $C_T$ and $C_P$), and $q(r)$ is the safety factor. The first contribution, i.e. the term $D_Z \partial n_Z / \partial r$, is diffusion. The second contribution, i.e. the term in $C_T$, corresponds to thermo-diffusion. The third contribution, i.e. the term in $C_P$, is due to curvature and is often called curvature pinch. The goal is to investigate these three contributions, and the dependancies of $D_Z$, $C_T$ and $C_P$, independantly of each others. Note that roto-diffusion is not included in our model.

Firstly, we isolate diffusion. We impose flat impurity temperature profiles to eliminate thermo-diffusion, and we artificially switch off curvature drift in the model to eliminate curvature pinch. We choose five different impurities with the same mass number ($A = 20$) but with 5 different charge numbers $Z$ from 2 to 12. We describe how impurity diffusive transport depends on the charge number, depending on the nature of the dominant instabilities: the diffusion coefficient increases with $Z$ in the case of TEM turbulence (Fig. 2), while it decreases with $Z$ in TIM-dominated turbulence, in good agreement with quasilinear theory. The dependency on mass number is much weaker [8].

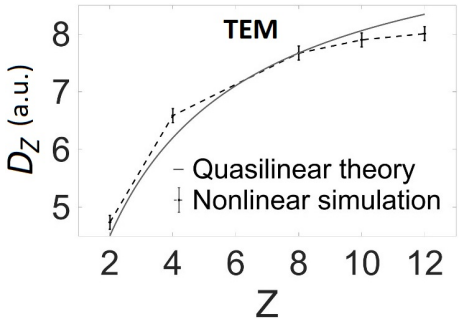


Figure 2: *Impurity diffusion coefficient versus impurity charge number Z (for TEM).*

Secondly, we isolate thermo-diffusion. Again we artificially switch off curvature drift in the model to eliminate curvature pinch. And since we cannot eliminate particle diffusion (a flat impurity density gradient cannot be maintained), we search for an impurity density gradient such that $\Gamma_Z = 0$. Then, $n_Z V_Z = -D_Z C_T \partial_r T_Z = D_Z \partial_r n_Z$, therefore $C_T = -\partial_r n_Z / \partial_r T_Z$. This procedure is applied for five different values of impurity temperature gradients. Fig. 3 shows that, as expected, the convection velocity $V_Z$ vanishes when the temperature profile

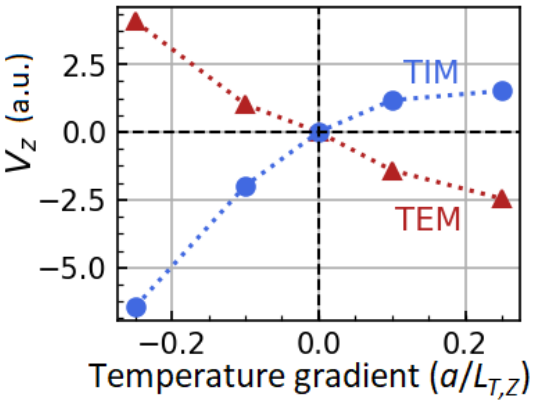


Figure 3: *Thermodiffusion velocity $V_Z$ versus impurity temperature gradient (TEM and TIM turbulences).*

is flat. $V_Z$ changes its sign when the temperature gradient does. We observe that the impurity pinch depends on the TIM or TEM nature of the turbulence. Here, $a/L_{T,Z} > 0$ means that the core is hotter than the edge, therefore the right part of the figure is more relevant for fusion plasmas. In this case, curvature pinch is inward except for reversed magnetic shear, consistently with Ref. [10].

Thirdly, we isolate the impurity density flux due to magnetic curvature pinch. We impose flat impurity temperature profiles to eliminate thermo-diffusion, and we focus near zero impurity density gradient. Then, $\Gamma_Z = n_Z V_Z = -D_Z C_P \partial_r q$. The Maxwellian distribution function $F_{eq}$,

$$F_{eq} = \frac{N_{eq}}{T_{eq}^{3/2}} \exp\left(-\frac{H_{eq}}{T_{eq}}\right) \qquad (2)$$

contains the effect of magnetic curvature through the radial dependency of the Hamiltonian $H_{eq} = (1 + e\Omega_d \psi) E$, where $\Omega_d E$ is the toroidal precession frequency, $\psi$ is the magnetic flux acting as a radial coordinate, and $E$ is the kinetic energy. Therefore, we can manipulate magnetic curvature by introducing an artificial scaling factor $\alpha$ such that $H_{eq} = (1 + e\alpha\Omega_d \psi) E$. A positive (negative) value of $\alpha$ mimics a positive (negative) magnetic shear. Fig. 4 shows the impurity density flux against density gradient for different values of $\alpha$. The flux is inward for positive magnetic shear (curvature pinch), while negative magnetic shear switches the sign of flux and prevents impurity core accumulation, in qualitative agreement with quasilinear theory.

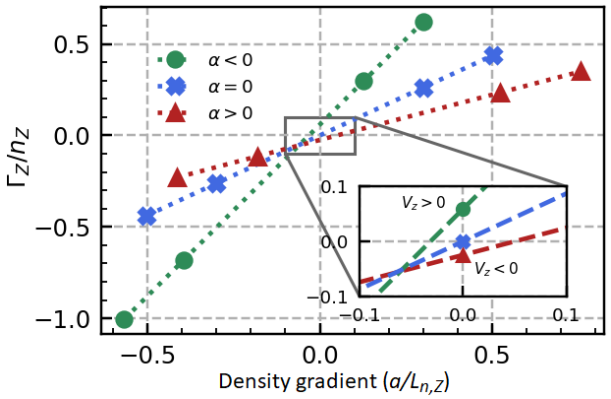


Figure 4: *Impurity density flux for a flat impurity temperature profile, against impurity density gradient, for different values of* $\alpha$. *The sign of* $\alpha$ *is representative of the sign of magnetic shear. For each curve, the intercept with the y-axis provides the flux due to magnetic curvature.*

## References


[1] M. Lesur, et al., Phys. Plasmas **24**, 012511 (2017)

[2] J. Médina, et al., Phys. Plasmas **25**, 122304 (2018)

[3] J. Médina, et al., Phys. Plasmas **26**, 102301 (2019)

[4] M. Idouakass, et al., Phys. Plasmas **25**, 062307 (2018)

[5] M. Lesur, et al., Nucl. Fusion **60**, 036016 (2020)

[6] H. Du, et al., Phys. Plasmas **21**, 052101 (2014).

[7] H. Du, et al., Phys. Plasmas **23**, 072106 (2016).

[8] E. Gravier, et al., Phys. Plasmas **26**, 082306 (2019)

[9] K. Lim, et al., Plasma Phys. Control. Fusion **62**, 095018 (2020).

[10] S. Futatani, et al., Phys. Rev. Lett. **104**, 015003 (2010).